ILMU KELAUTAN: Indonesian Journal of Marine Sciences *September 2026 Vol 31(3):309-322* *e-ISSN 2406-7598*

Coastal Vulnerability Assessment and Disaster Risk Management of the Betahwalang Conservation Area, Demak, Indonesia

Agus Indarjo[1], Galung Dhiva Maharani[1,3,4], Muhammad Zainuri[2,3,4]*, Hadi Endrawati[1], Suryono[1]

[1]Department of Marine Science, Faculty of Fisheries and Marine Science, Universitas Diponegoro
[2]Department of Oceanography, Faculty of Fisheries and Marine Science, Universitas Diponegoro
Jl. Prof. Jacub Rais, Tembalang, Semarang, Central Java, 50275 Indonesia
[3]Center for Coastal Rehabilitation and Disaster Mitigation Studies, Universitas Diponegoro
[4]Integrated Laboratory for Research and Services, Diponegoro University
Jl. Prof. Soedarto, SH, Tembalang, Semarang, Central Java, 50275 Indonesia
Email: muhammadzainuri@lecturer.undip.ac.id

Abstract

Low-lying coastal regions worldwide face escalating threats from sea-level rise, land subsidence, coastal erosion, and recurrent tidal flooding, underscoring the urgent need for effective disaster management informed by spatial vulnerability assessments. This study evaluates temporal changes in coastal vulnerability within Betahwalang Waters, Demak Regency, Indonesia, over the period 2015–2025, applying the Coastal Vulnerability Index (CVI) integrated with Geographic Information Systems (GIS). Primary data were obtained through field surveys, whereas secondary data comprised Sentinel-2 satellite imagery, digital elevation and bathymetric datasets, and tidal records. Coastal vulnerability was analyzed using a GIS-based weighted overlay approach that combined and quantified multiple physical, geological, and environmental parameters. The results reveal that approximately 69% of the study area falls within the high to very high vulnerability categories, with geomorphology and coastal slope emerging as the two dominant contributing factors, each accounting for 20% of the overall index. A comparison with the 2015 BNPB coastal hazard assessment indicates a pronounced spatial expansion of high-vulnerability coastal zones over the past decade, primarily driven by tidal inundation, aquaculture expansion, and progressive mangrove degradation. This study contributes to coastal disaster management by demonstrating the value of integrating field observations, remote sensing, and GIS for monitoring long-term vulnerability dynamics. The findings offer a robust scientific basis for disaster risk reduction, vulnerability-based spatial planning, and ecosystem-based coastal management. Collectively, they provide a practical and transferable framework for strengthening the resilience of tropical deltaic coasts confronting intensifying climate-related hazards in similarly vulnerable low-lying coastal environments worldwide.

Keywords: *Coastal Vulnerability Index, Tidal Flooding, Betahwalang, Demak, Resilience*

Introduction

Coastal regions are among the most productive yet vulnerable environments on Earth. In Indonesia—an archipelagic nation with over 80,000 km of coastline—these zones are vital for economic activity, fisheries, agriculture, and settlement. However, coastal areas are increasingly threatened by natural and anthropogenic pressures such as sea-level rise, tidal flooding (rob), erosion, and land subsidence. The northern coast of Java (Pantura) exemplifies this situation, where rapid environmental change, driven by climatic variability and human exploitation, has intensified the degradation of coastal ecosystems and increased disaster risk. Demak Regency in Central Java is one of the most critical coastal areas within this region. Its coastline is dominated by flat alluvial plains that function as aquaculture ponds, rice fields, and residential zones—land uses that are highly sensitive to coastal hazards (Dewi *et al*., 2017; Carvalho *et al*., 2025). The area's geomorphology, combined with excessive groundwater extraction and poorly managed land-use expansion, has contributed to significant land subsidence and recurring tidal inundation. These processes not only threaten physical infrastructure but also undermine local livelihoods and regional economic stability. The coastal dynamics of Demak are influenced by seasonal monsoonal variability, which affects wave conditions, sediment transport, and shoreline processes. These seasonal processes contribute to long-term coastal changes that, together with land

*) Corresponding author

https://ejournal.undip.ac.id/index.php/ijms
DOI: 10.14710/ik.ijms.31.3.309-322
Received : 14-05-2026
Accepted : 16-07-2026

subsidence and anthropogenic pressures, increase the vulnerability of the study area.

Betahwalang Village (S 6°48'12.22"–6°47' 1.97" and E 110°32'22. 93"–110°33'42.5"), located in Bonang District, exemplifies these challenges. It is an ecologically and socioeconomically important coastal area that supports small-scale fisheries and aquaculture. However, over the past ten years, Betahwalang has faced intensified environmental stress manifested in tidal inundation, coastal erosion, and land loss. The rapid conversion of mangrove ecosystems into aquaculture ponds, combined with sea-level rise and sediment depletion, has accelerated vulnerability in this area (Fithor *et al*., 2021; Fiorucci *et al*., 2022; Estradas-Romero *et al*., 2025). A comparison of coastal vulnerability between 2015 and 2025 reveals a marked deterioration in environmental conditions. The 2015 flood hazard map produced by the Indonesian National Disaster Management Agency (BNPB) provided an overview of coastal vulnerability across Demak Regency. At that time, most of the coastal subdistricts—especially Sayung, Wedung, and Karangtengah—were classified as moderate to high in vulnerability, while southern areas were relatively less exposed. By contrast, the 2025 analysis, based on in-situ observations and high-resolution spatial data, shows a significant escalation in risk levels. Nearly the entire coastal zone of Betahwalang now falls within high to very high vulnerability categories, with extreme susceptibility along the shoreline and river mouths. This shift indicates that coastal hazards have become more spatially extensive and severe, driven by the cumulative impacts of tidal flooding, shoreline retreat, and ineffective land-use control. To systematically evaluate such changes, the Coastal Vulnerability Index (CVI) provides a valuable analytical framework. The Coastal Vulnerability Index (CVI) integrates multiple physical and environmental parameters into a composite index to quantify coastal vulnerability. In this study, the CVI incorporates geomorphology, coastal slope, elevation, distance from the shoreline, distance from rivers, tidal range, and land use, representing the primary factors controlling coastal susceptibility in the Betahwalang coastal system. Integrating these parameters within a GIS environment enables spatially explicit identification of vulnerable coastal areas and supports long-term monitoring of vulnerability dynamics. In application to multi-temporal datasets, the CVI method effectively captures how physical and environmental conditions evolve over time. This approach supports spatially explicit risk assessments, enabling policymakers and planners to identify critical zones that require immediate adaptation or mitigation measures. The increasing CVI values observed in Betahwalang from 2015 to 2025 underscore the limited effectiveness of existing coastal management efforts. Structural measures such as embankment construction and drainage improvements have been implemented, but these remain insufficient without ecosystem-based and community-centered strategies. Previous initiatives—including mangrove rehabilitation programs and fishery conservation efforts supported by local regulations (*e.g.,* Demak District Regulation No.523/0166/2014)—have contributed to partial improvements but have not significantly reduced overall vulnerability. The persistence of high-risk conditions indicates the need for an integrated approach that combines structural, ecological, and social resilience-building. The application of remote sensing and GIS-based techniques further enhances the CVI assessment by providing continuous and spatially comprehensive data across different seasons. Given the tropical climatic variability of the North Java coast, seasonal observations—during both the east and west monsoons—are crucial to capture dynamic coastal responses. Integrating these spatial datasets with CVI modeling allows for more precise identification of vulnerable zones and helps to monitor long-term environmental trends.

Although previous studies have documented coastal flooding, shoreline change, land subsidence, and mangrove degradation along the Demak coast, most investigations have focused on individual coastal processes or single-period assessments. Comprehensive evaluations that quantify how coastal vulnerability has evolved over a decadal timescale using a consistent CVI framework remain limited. Furthermore, previous studies rarely identify the relative contribution of individual vulnerability parameters to the observed changes, limiting their applicability for evidence-based disaster management and long-term coastal planning.

Therefore, this study aims to analyze and compare the coastal vulnerability of Demak Regency between 2015 and 2025 using the Coastal Vulnerability Index (CVI) method. The specific objectives are: (a) to assess the spatial distribution of coastal vulnerability in Betahwalang Waters, Demak; (b) to categorize the vulnerability levels based on CVI parameters; and (c) to determine the parameters with the greatest and least influence on the overall vulnerability score. By conducting a decadal comparison, this study provides empirical evidence of the evolving vulnerability pattern in Demak and highlights the urgency of adaptive coastal management. The results of this research are expected to contribute to the formulation of more sustainable and resilient coastal spatial planning strategies in Demak Regency and the broader North Java region. The study underscores the importance of integrating CVI-based vulnerability assessments into regional development and disaster mitigation policies. Through this approach, decision-makers can design spatially adaptive plans that balance economic activities with environmental sustainability, thus ensuring the long-term resilience of coastal communities against the growing threats of climate change and anthropogenic degradation.

The scientific contribution of this study lies in its decadal assessment of coastal vulnerability using a consistent CVI framework integrated with field observations, remote sensing, and GIS analysis. Unlike previous studies that primarily evaluated coastal vulnerability at a single point in time, this research quantifies temporal changes in vulnerability over a ten-year period while identifying the dominant physical factors responsible for these changes. This approach provides a more robust basis for evaluating the effectiveness of previous coastal management efforts and supports adaptive disaster risk reduction under ongoing climate and land-use change.

Based on the increasing impacts of tidal flooding, land subsidence, shoreline retreat, and mangrove degradation observed over the last decade, this study hypothesizes that the coastal vulnerability of Betahwalang has significantly increased between 2015 and 2025. It is further hypothesized that geomorphology and coastal slope are the dominant factors influencing the Coastal Vulnerability Index (CVI) compared to other physical parameters.

Materials and Methods

Data sources and field survey

This research utilized both primary and secondary data to assess coastal vulnerability in Betahwalang Waters, Demak. Primary data were collected through a field survey conducted in April 2025, during the first transitional monsoon season (Figure 1). A total of 57 observation stations were distributed purposively along the Betahwalang coastline to represent variations in coastal geomorphology, land use, and shoreline characteristics. At each observation station, geomorphological conditions, vegetation types, and the presence of coastal protection structures, including mangroves and embankments, were recorded to support geomorphological classification and validate spatial interpretation (Capobianco *et al*., 2016; Pasomba *et al*., 2019; Furlan *et al*., 2021; Ariffin *et al*., 2023). The survey was conducted as a single field campaign because the objective of the study was to characterize the spatial distribution of coastal vulnerability rather than to evaluate temporal variability.

Coastal slope measurements were conducted at each observation station using a Real-Time Kinematic Global Navigation Satellite System (RTK-GNSS E-Survey). Measurements were performed along a shore-normal transect extending from the lowest tidal point to the nearest vegetation line, with an average transect length of approximately 50 m, depending on local coastal conditions. The horizontal distance and corresponding elevation difference between the two endpoints were recorded to calculate the coastal slope (Fadika *et al*., 2014; Ervianto and Hariyanto, 2021). Each station was measured once because the objective was to characterize the spatial variability of coastal slope across the study area rather than to evaluate temporal measurement variability. To ensure data quality, measurements were recorded only after the RTK receiver indicated zero positioning error on the instrument display, thereby minimizing positional uncertainty. The resulting slope values were subsequently used to classify the coastal slope parameter within the Coastal Vulnerability Index (CVI) framework.

Secondary data included Sentinel-2 satellite imagery, digital elevation models (DEM), bathymetric data, and tidal records obtained from the Meteorological, Climatological, and Geophysical Agency (BMKG). Sentinel-2 imagery was used to delineate the shoreline and derive land-use information, while bathymetric and DEM datasets supported elevation analysis. Tidal records were used to calculate the average tidal range incorporated into the CVI analysis.

Data pre-processing

All satellite data were pre-processed before analysis. Sentinel-2 imagery was atmospherically corrected using the Semi-Automatic Classification Plugin (SCP) in ArcGIS 10.8 to minimize haze and cloud interference. Images with less than 10% cloud cover were selected to ensure high-quality visual data. The Normalized Difference Water Index (NDWI) was applied to enhance the contrast between land and water surfaces and accurately delineate the shoreline (Hopper and Meixler, 2016; Hammar *et al*., 2003; Sagala *et al*., 2024). DEM data were corrected by resampling to a uniform 10-meter resolution to maintain spatial consistency across layers. Tidal data were averaged over a one-year period (2024-2025) to represent typical tidal fluctuations and avoid seasonal bias.

Spatial analysis and software

Spatial analysis was conducted using ArcGIS 10.8 (Esri Inc.) and Microsoft Excel 2021 for statistical tabulation and calculations. Geospatial analyses, including shoreline delineation, distance measurements, raster reclassification, and weighted overlay analysis, were performed within the ArcGIS environment (Gornitz, 1991; Handayani *et al*., 2024; Ledheng *et al*., 2024). All spatial datasets were projected using the Universal Transverse Mercator (UTM) coordinate system, Zone 49S, referenced to the WGS 84 datum. Each of the six physical parameters—geomorphology (G), coastal slope (S), elevation (E), distance from shoreline (DfS), distance from rivers (DfR), and tidal range (TR)—together with one anthropogenic parameter (land use, LU), was digitized and classified according to the vulnerability thresholds presented in Table 1. The classified parameters were subsequently standardized into vulnerability scores ranging from 1 (very low vulnerability) to 5 (very high vulnerability) prior to the weighted overlay analysis for CVI calculation.

Weighting and rationale

The weighting of each parameter was determined based on its relative influence on coastal processes, following previous studies (Darmawan *et al*., 2017; Pantusa *et al*., 2018; Ramadhany *et al*., 2021). Geomorphology (20%) and slope (20%) received the highest weights as they directly determine the physical resistance of the coastline to erosion and inundation. Steeper

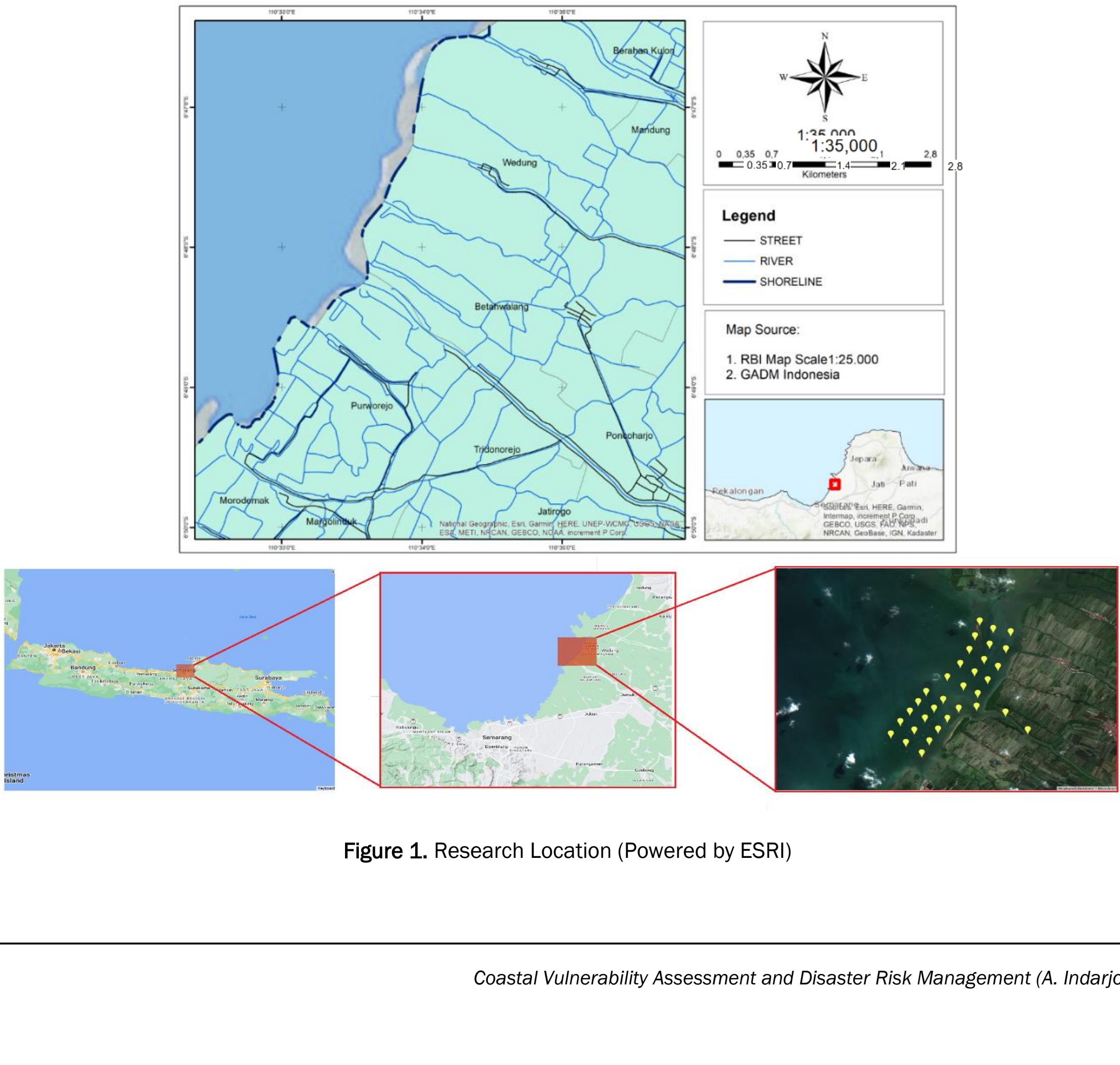

Figure 1. Research Location (Powered by ESRI)

slopes and rocky coasts generally indicate lower vulnerability, whereas flat deltaic and sandy coasts are more prone to flooding and erosion. Elevation (15%), distance from shoreline (15%), and distance from river (15%) were given moderate weights because these parameters influence the degree of exposure to hydrodynamic forces and fluvial processes. Tidal range (10%) was weighted slightly lower since its effect is periodic but still contributes to wave energy distribution and inundation frequency. Land use (5%) received the lowest weight because anthropogenic characteristics tend to modify, but not fundamentally determine, the physical vulnerability of coastal systems. However, it remains relevant for identifying areas with artificial reinforcement (*e.g.,* settlements, fish ponds).

Prior to the weighted linear combination (WLC) analysis, all parameter layers were standardized through a reclassification process based on the vulnerability classes presented in Table 1. Continuous variables, including coastal slope, elevation, distance from shoreline, distance from rivers, and tidal range, were classified into five ordinal vulnerability scores ranging from 1 (very low vulnerability) to 5 (very high vulnerability). Categorical variables, such as geomorphology and land use, were directly assigned to the corresponding vulnerability classes according to their physical characteristics. Consequently, no additional mathematical normalization (*e.g.,* min–max or z-score normalization) was applied, as all parameters had already been converted to a common ordinal scale prior to weighting. Extreme values were accommodated within the predefined classification thresholds, ensuring that outliers did not disproportionately influence the final CVI score.

This weighting scheme ensures that dominant geomorphological and topographical features have a proportionally larger impact on the computed CVI value than secondary or human-induced factors. Computation of the Coastal Vulnerability Index (CVI) The Coastal Vulnerability Index was calculated using a weighted linear combination (WLC) model based on the formula (Darmawan *et al*., 2017; Pantusa *et al*., 2018; Ramadhany *et al*., 2021):

(1) $CVI = \Sigma Wi \times Si = (20 \times G) + (20 \times S) + (15 \times E) + (15 \times DfS) + (15 \times DfR) + (10 \times TR) + (5 \times LU)$

Note: CVI= Coastal Vulnerability Index; Wi= weight assigned to each parameter i (expressed as a percentage); Si= score representing the vulnerability class of each parameter; G= geomorphology; S= slope; E= elevation; DfS= distance from shoreline; DfR= distance from river; TR= tidal range; LU= land use.

The resulting CVI values were categorized into five vulnerability levels: very low, low, medium, high, and very high, using natural break classification within ArcGIS. Each spatial cell was then color-coded according to its vulnerability level to generate the final coastal vulnerability map for Betahwalang Waters.

Because the study applies a GIS-based weighted overlay model instead of predictive modelling, regression analysis was not appropriate. To improve the methodology, uncertainty and field validation have been described in greater detail.

Validation and accuracy

To ensure the reliability of the spatial outputs, field observations were cross-referenced with the CVI results. High-vulnerability areas (red zones) corresponded closely with observed tidal inundation sites and areas of active erosion, confirming the accuracy of model predictions.

Table 1. Score and weight for each coastal vulnerability criterion

Variables	Score					Weight
	Very Low 1	Low 2	Medium 3	High 4	Very High 5	
Geomorphology (G)	Stony and hilly beach	Medium clifffed beach	Low cliffed-beach, glacial flow	Stony beach, estuary, lagoon	Barrier beach, sandy beach, delta	20%
Slope (S)	>12%	8 - 12%	4 - 8%	2 - 4%	<2%	20%
Elevation (E)	>3.4 m	3.0 - 3.4 m	2.5 - 3.0 m	1.8 - 2.5 m	<1.8 m	15%
Distance from shoreline (DfS)	>1000 m	750 - 1000 m	500 - 750 m	250 - 500 m	0 - 250 m	15%
Distance from River (DfR)	>400 m	300 - 400 m	200 - 300 m	100 - 200 m	0 - 100 m	15%
Tidal Range (TR)	<0.2 m	0.2 - 0.4 m	0.4 - 0.6 m	0.6 - 0.8 m	>0.8 m	10%
Land use (LU)	Mangrove forest	Plantation, farm	Open Field, scrub	Built land, house, buildings	River, pond	5%

Source: Darmawan *et al*. (2017); Pantusa *et al*. (2018); Ramadhany *et al*. (2021)

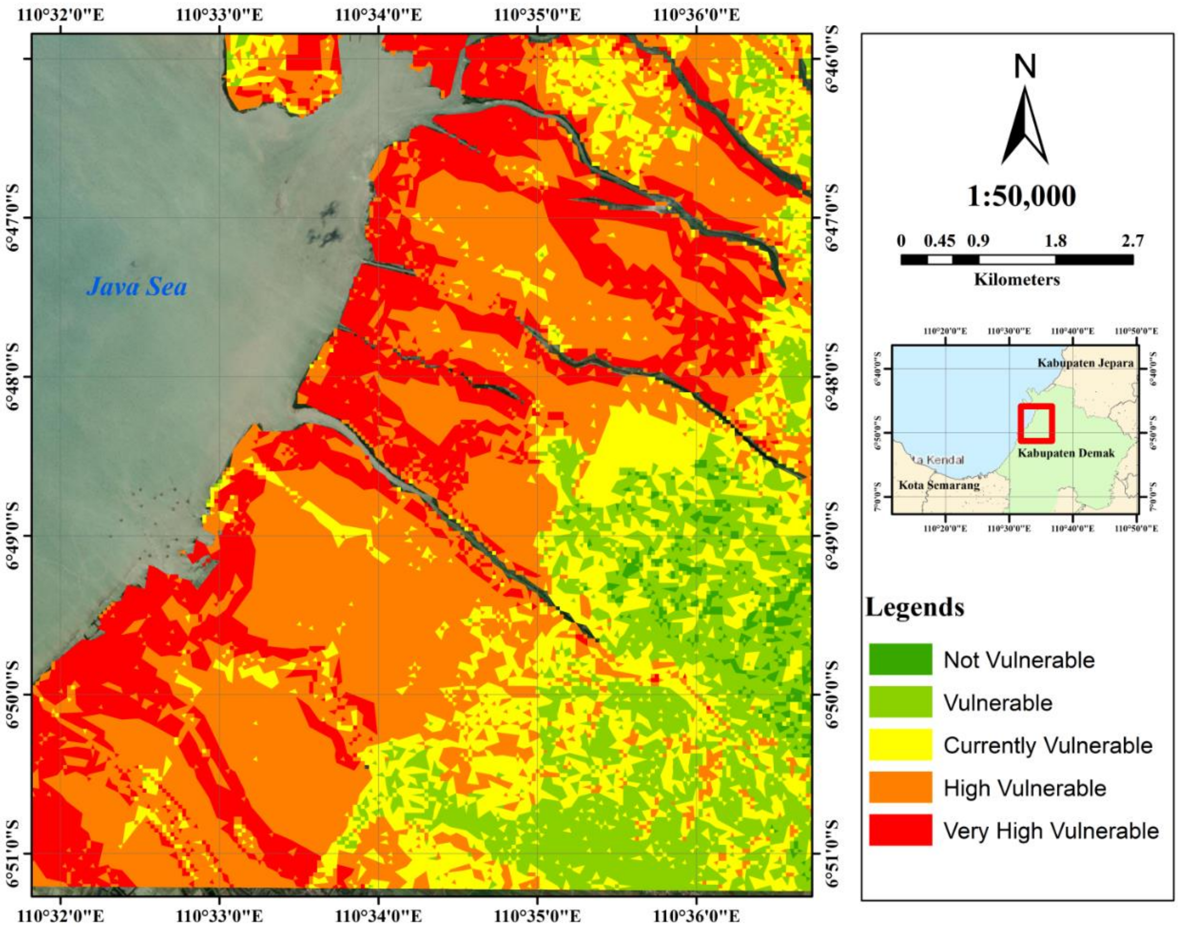

Figure 3. Vulnerability Map of Demak Regency in 2025

Statistical validation was conducted by comparing the computed CVI values with historical flood event records and geomorphological observations across the study area (Macedo and Schettini, 2025; Muliati, 2020).

Results and Discussion

The CVI is a tool used to measure the susceptibility of coastal areas to various threats, including sea-level rise, erosion, tidal flooding, and saltwater intrusion. This method integrates multiple physical and environmental parameters into a single index value, which is then classified into categories—Not Vulnerable, Low, Medium, High, and Very High—to support interpretation and planning. The following figures present the processed results of each parameter: geomorphology, land use, elevation, slope, distance from the coast, distance from rivers, and tidal range (Ningtias *et al*., 2016; Oktaviani and Kusuma, 2017). These parameters were analyzed using a weighted overlay technique to produce the final coastal vulnerability map.

Spatial distribution of coastal vulnerability

The spatial analysis of flood vulnerability in Demak Regency reveals significant changes over the past decade. The 2015 flood hazard map depicted vulnerability at the regency scale, with high to very high levels concentrated in the northern coastal districts such as Sayung, Wedung, and Karangtengah. This distribution corresponds to Demak's geomorphological features, dominated by low-lying alluvial plains prone to both riverine floods and tidal inundation. In contrast, the southern districts bordering Semarang and Grobogan exhibited lower vulnerability due to higher elevations and less direct influence from tidal dynamics. Overall, the 2015 assessment presented a varied distribution of vulnerability, ranging from medium to high in coastal areas and low to medium inland. By 2025, the localized analysis in Betahwalang Village, Bonang District, shows a marked escalation of vulnerability. The map presented in Figure 3 (Vulnerability Map of Demak Regency in 2025) was produced by the authors. The Digital Elevation Model (DEM) was entirely collected independently by the authors and processed using ArcGIS software, with spatial layers obtained from public-domain data provided by the Ina-Geoportal. Nearly the entire coastal zone is now categorized as high to very high, with the most critical areas found along shorelines and river mouths (Rudiarto *et al*., 2016; Primasti *et al*., 2021). The dominance of red zones in the 2025 map indicates severe vulnerability that was previously only localized in 2015 but has since expanded spatially. Only a small portion of inland areas remains at medium to low vulnerability. This transformation highlights the cumulative effects of environmental degradation processes such as coastal abrasion, recurrent tidal flooding, land subsidence, and sea-level rise, which have intensified the risks in Demak's coastal landscape. The comparison between the 2015 and 2025 maps underscores the sharp escalation of flood vulnerability in Demak's coastal areas. While the 2015 map served primarily as a regional-scale instrument for identifying risk, the 2025 map provides a more detailed local perspective that emphasizes the urgency of intervention. The expansion of high to very high vulnerability zones reflects both natural and anthropogenic pressures that have overwhelmed existing coastal management practices. This shift demonstrates the increasing severity of climate-related hazards and the growing exposure of communities living in low-lying coastal zones. The spatial analysis of the Coastal Vulnerability Index (CVI) in Betahwalang Waters, Demak, reveals a clear concentration of high to very high vulnerability zones along the shoreline and estuarine areas. Based on the weighted

Table 2. Potential Population Exposure to Floods in Demak Regency in 2015

No	District	Exposed Population (People)	Vulnerable groups (People)			Vulnerability Class
			Vulnerable Age Population	Poor Population	Disabled Population	
1	Mranggen	165,089	24,114	33,015	526	High
2	Karangawen	83,612	12,213	36,553	345	High
3	Guntur	73,563	10,745	35,089	302	High
4	Sayung	101,025	14,756	34,087	287	High
5	Karang Tengah	60,925	8,899	19,166	239	High
6	Bonang	98,918	14,449	47,818	265	High
7	Demak	99,917	14,595	21,863	389	High
8	Wonosalam	71,363	10,424	22,285	222	High
9	Dempet	51,445	7,514	22,718	168	High
10	Kebonagung	26,927	3,933	11,003	232	High
11	Gajah	43,521	6,357	14,059	227	High
12	Karanganyar	64,976	9,491	17,839	306	High
13	Mijen	50,519	7,379	18,285	120	High
14	Wedung	72,240	10,552	31,696	679	High
Demak Regency		1,064,040	155,421	365,476	4,307	High

Table 3. Potential Population Exposure to Extreme Weather Disasters in Demak Regency in 2015

No	District	Exposed Population (People)	Vulnerable groups (People)			Vulnerability Class
			Vulnerable Age Population	Poor Population	Disabled Population	
1	Mranggen	166,548	24,327	33,346	534	High
2	Karangawen	85,737	12,523	37,360	351	High
3	Guntur	73,503	10,736	35,060	302	High
4	Sayung	100,760	14,718	33,992	287	High
5	Karang Tengah	60,918	8,898	19,163	239	High
6	Bonang	98,926	14,450	47,823	265	High
7	Demak	99,917	14,595	21,863	389	High
8	Wonosalam	71,363	10,424	22,285	222	High
9	Dempet	51,383	7,505	22,686	168	High
10	Kebonagung	26,799	3,914	10,950	231	High
11	Gajah	43,510	6,355	14,057	227	High
12	Karanganyar	64,949	9,487	17,836	306	High
13	Mijen	50,648	7,398	18,335	120	High
14	Wedung	72,196	10,545	31,667	678	High
Demak Regency		1,067,157	155,875	366,423	4,319	High

overlay results, five vulnerability categories were identified: very high (>3.95), high (2.37–3.95), medium (1.55–2.37), low (0.8–1.55), and not vulnerable (<0.8). The total area classified as very high vulnerability reached approximately 1,585.7 ha (26.0%), while high vulnerability covered 2,615.3 ha (42.9%) of the total study area. In contrast, medium and low vulnerability zones accounted for 13.2% and 17.3%, respectively, whereas non-vulnerable areas comprised less than 1% (Table 3). The CVI analysis indicates that approximately 69% of the Betahwalang coastal area falls within the high to very high vulnerability categories, highlighting widespread physical susceptibility to coastal hazards. Although the comparison with the 2015 BNPB coastal hazard assessment suggests a substantial spatial expansion of vulnerable areas, the two assessments were developed using different datasets, methodologies, and spatial resolutions. Therefore, the comparison should be interpreted qualitatively as evidence of long-term changes in coastal conditions rather than as a statistically comparable temporal assessment. When compared to the 2015 regional-scale analysis of Demak Regency by BNPB, which already classified the entire regency as "high vulnerability," the 2025 local-scale CVI map demonstrates a significant intensification and spatial expansion of critical zones (Sugianto and Muhammad 2019; Sousa *et al*., 2025). While in 2015 the vulnerable areas were concentrated mainly in northern districts such as Sayung and Wedung, by 2025 the Betahwalang coastline shows a broader and more severe pattern of vulnerability. This reflects the cumulative impacts of tidal flooding, land subsidence, shoreline retreat, and mangrove loss over the past decade.

It should be noted that the comparison between the 2015 BNPB coastal hazard assessment and the 2025 CVI-based vulnerability assessment should be interpreted with caution, as the two datasets differ in their objectives, methodologies, data sources, and spatial resolution. The 2015 BNPB map was developed as a regional hazard assessment using government datasets, whereas the present study employs a field-validated CVI framework integrated with remote sensing and GIS to evaluate coastal vulnerability at a finer spatial scale. Therefore, the comparison is intended to illustrate the overall spatial evolution of coastal vulnerability over the past decade rather than to provide a direct quantitative equivalence between the two assessments. Despite these methodological differences, both datasets consistently indicate increasing vulnerability along the Demak coast, supporting the interpretation of a progressive deterioration in coastal conditions.

Parameter contribution to coastal vulnerability

The relative contribution of each parameter, based on its weight and score distribution, highlights geomorphology and slope as the dominant drivers, each contributing 20% to the total CVI score. The geomorphological setting of Betahwalang—composed mainly of barrier beaches and deltaic plains—represents a soft, easily erodible substrate highly sensitive to wave action and tidal inundation (Sunaryo *et al*., 2017; Suryono *et al*., 2018; Tomasi and Klein, 2025). The slope parameter further amplifies this vulnerability, as much of the study area exhibits a gentle gradient of less than 2%, promoting prolonged water retention and inundation. Elevation (15%) also plays a significant role. More than half of the area lies below 2 m above mean sea level, corresponding to high to very high elevation scores. The distance from shoreline (DfS) and distance from river (DfR) parameters (each 15%) contributed moderately, with zones within 250 meters of the shoreline or 100 m of river channels classified as highly vulnerable due to direct exposure to tidal and fluvial interactions. The tidal range (TR) parameter, with a 15% weight, reflects the influence of hydrodynamic forces on coastal morphology. Betahwalang experiences a mean tidal range of 0.8–1.0 m, placing much of the area in the "high" vulnerability class. The land use (LU) variable, although weighted lowest at 5%, still provides meaningful insight: areas dominated by fish ponds and open water corresponded to higher vulnerability, while vegetated or mangrove-covered zones showed lower CVI values. However, mangrove density was represented categorically (not quantitatively), which may understate its actual protective function. Previous studies (*e.g.*, Irsadi *et al*., 2019; Furlan *et al*., 2021) emphasize that mangrove canopy density, root biomass, and width of mangrove belts substantially reduce wave energy and erosion risk—suggesting that future models should include vegetation density as a continuous parameter.

Comparison with previous studies

The findings of this study are consistent with previous Coastal Vulnerability Index (CVI)-based assessments conducted across Indonesia and Southeast Asia while providing quantitative evidence of increasing vulnerability in the Betahwalang coastal area. Approximately 69% of the study area was classified as having high to very

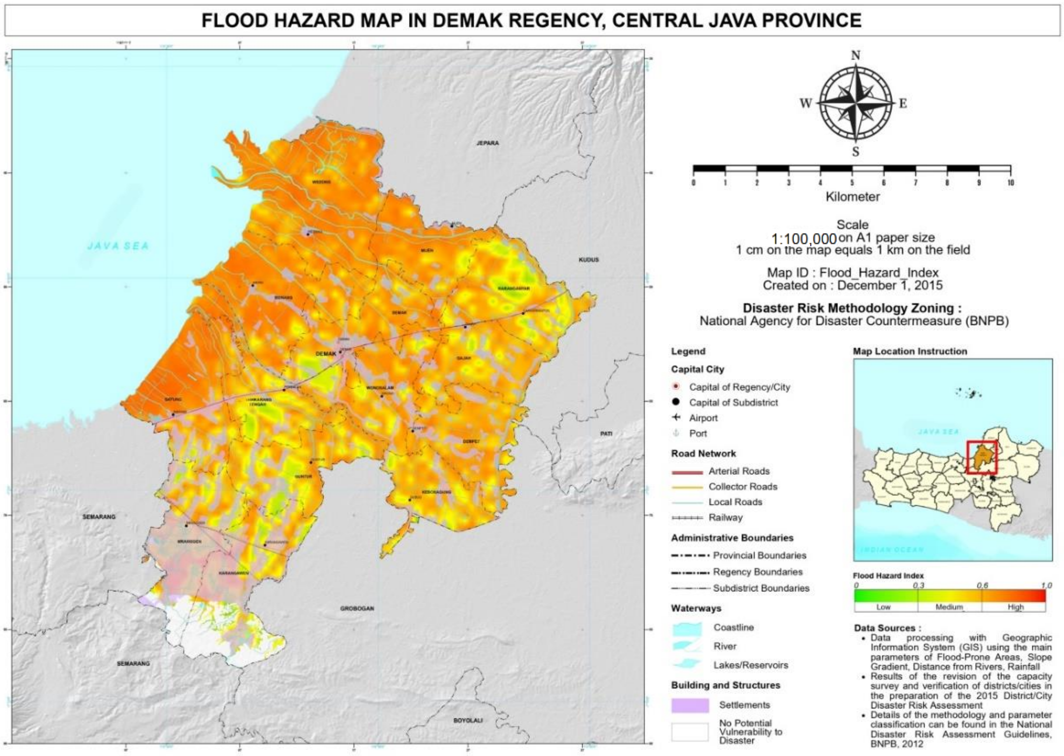

a

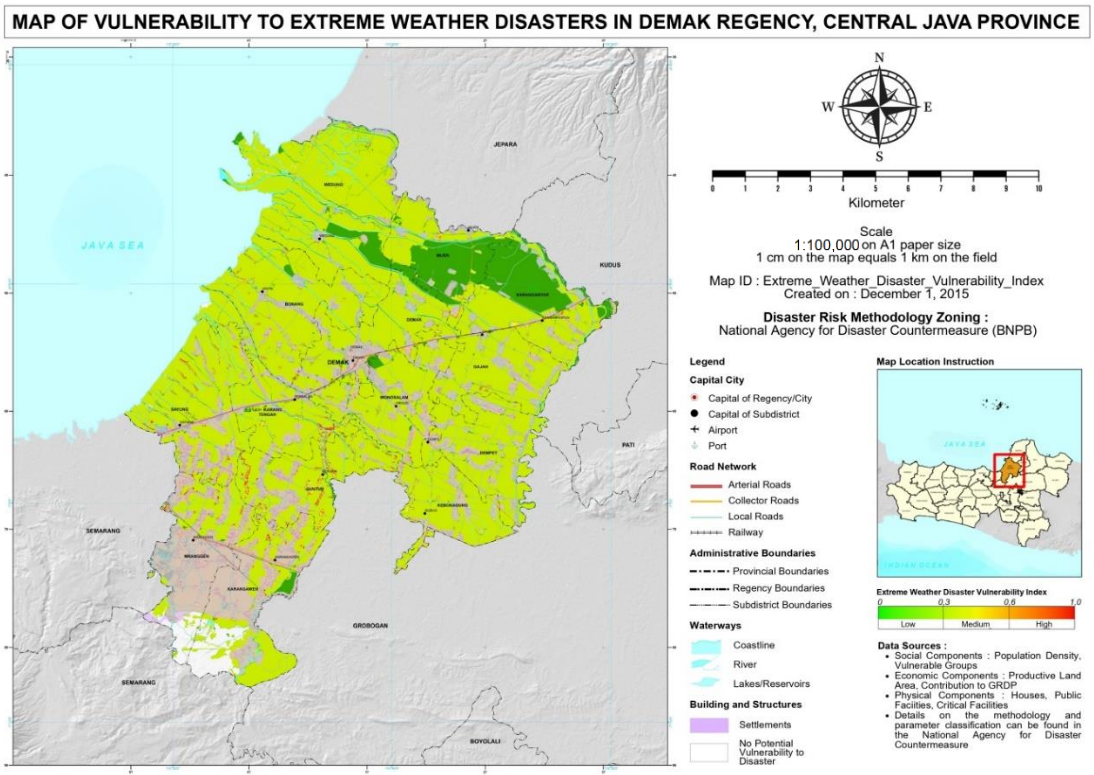

b

Figure 2. Vulnerability Map of Demak Regency in 2015: a) Based on Floods; b) Based on Extreme Weather

high vulnerability, indicating a substantial concentration of coastal risk. This result is comparable to previous studies that identified low-lying coastal plains as the most vulnerable environments. Darmawan *et al*. (2017) reported that geomorphology and elevation were the dominant factors controlling flood vulnerability in Sampang, Madura, while Ramadhany *et al*. (2021) similarly demonstrated that flat coastal areas with intensive anthropogenic land use were highly susceptible to tidal inundation in Semarang. Likewise, Pantusa *et al*. (2018) and Arini *et al*. (2014) showed that deltaic and low-elevation coastal environments experienced rapid increases in vulnerability due to the combined effects of sea-level rise, coastal erosion, and land subsidence. The results obtained for Betahwalang support these findings, where geomorphology and slope emerged as the dominant contributors to the CVI, together accounting for 40% of the total weighting, while extensive aquaculture development and mangrove degradation further increased coastal exposure. Compared with the regional-scale flood hazard assessment conducted by BNPB in 2015, which generally classified the Demak coastal region as highly vulnerable, the present study provides a more detailed local-scale assessment demonstrating the spatial expansion and intensification of high-risk zones over the past decade. The consistency of these findings across different geographic settings confirms the robustness of the CVI framework for assessing coastal vulnerability while emphasizing the importance of local-scale analyses for identifying priority areas requiring intervention.

From a coastal management perspective, these findings have important policy implications. The concentration of high and very high vulnerability zones along the shoreline and estuarine areas suggests that coastal management strategies should prioritize ecosystem-based adaptation alongside conventional engineering measures. Strengthening mangrove rehabilitation, protecting remaining coastal vegetation, regulating aquaculture expansion in highly exposed areas, and incorporating CVI-based vulnerability maps into coastal spatial planning and disaster risk reduction programs would improve long-term coastal resilience. Furthermore, periodic updates of vulnerability assessments using geospatial monitoring can support evidence-based decision-making and enable local governments to develop adaptive management strategies that respond to ongoing environmental change and increasing climate-related coastal hazards.

Beyond the physical characteristics of coastal vulnerability, the findings also have important socio-economic implications for coastal communities in Betahwalang. The predominance of high and very high vulnerability zones indicates increasing exposure of aquaculture ponds, fisheries infrastructure, settlements, and supporting public facilities to recurrent tidal flooding and coastal erosion. These conditions may reduce aquaculture productivity, disrupt local livelihoods, increase maintenance and rehabilitation costs, and ultimately weaken community resilience. Integrating CVI-based vulnerability assessments into local development planning can therefore support more effective allocation of resources, improve disaster preparedness, and strengthen adaptive capacity through ecosystem-based coastal management and sustainable land-use planning.

Role of mangrove ecosystems

Mangrove ecosystems play a crucial role in reducing coastal vulnerability by attenuating wave energy, stabilizing sediments, and protecting shorelines from erosion and tidal inundation. In Betahwalang, field observations and recent satellite imagery indicate that mangrove ecosystems have been locally fragmented and partially converted into aquaculture ponds, reducing their effectiveness as natural coastal buffers (Sugianto *et al*., 2019; 2022). Although this study did not quantify temporal changes in mangrove area, the observed degradation is consistent with previous studies reporting continued mangrove loss and increasing coastal exposure along the Demak coast. These findings emphasize the importance of mangrove conservation and restoration as ecosystem-based

Table 4. CVI Category Class in Betahwalang, Demak in 2025

CVI category	CVI Value	Area (Ha)	% of Area
Not Vulnerable	< 0.8	32.27	0.53
Low Vulnerability	0.8 – 1.55	1051.17	17.26
Medium Vulnerability	1.55 > CVI ≤ 2.37	803.71	13.2
High Vulnerability	2.37 > CVI ≤ 3.95	2615.26	42.95
Very High Vulnerability	> 3.95	1585.73	26.04

approaches for reducing coastal vulnerability. The absence of dense vegetation increases surface exposure to hydrodynamic forces, explaining the high CVI values along the pond edges. Rehabilitation of mangroves, especially species with strong root structures such as Rhizophora and Avicennia, is therefore vital to restoring coastal resilience.

Although vegetation indices such as the Normalized Difference Vegetation Index (NDVI) have been widely applied to assess vegetation greenness, they were not incorporated into the present study because the Coastal Vulnerability Index (CVI) framework adopted herein relies on standardized physical and land-use parameters. In this study, the protective role of mangrove ecosystems was represented through the land-use parameter, which distinguishes mangrove forests from other coastal land-cover types. Moreover, NDVI primarily reflects vegetation greenness and does not directly quantify the coastal protection capacity of mangroves, which is also influenced by ecological characteristics such as species composition, root structure, belt width, stand density, and forest age. Therefore, the land-use approach was considered appropriate for maintaining consistency with the selected CVI methodology and facilitating comparison with previous CVI-based studies.

Uncertainty and limitations

Despite providing valuable insights, this CVI model has several limitations. The analysis focused primarily on standardized biophysical and anthropogenic parameters within the adopted Coastal Vulnerability Index (CVI) framework, excluding socio-economic and hydrodynamic variables such as population density, infrastructure value, and wave energy, all of which may further influence coastal vulnerability and exposure. In addition, mangrove ecosystems were represented using a categorical land-use parameter rather than quantitative vegetation indices (*e.g.*, NDVI). This approach was adopted to maintain consistency with the selected CVI methodology and facilitate comparison with previous CVI-based studies. Although NDVI is useful for assessing vegetation greenness, it does not directly quantify the coastal protection function of mangroves, which is also influenced by ecological characteristics such as species composition, stand density, belt width, root structure, and forest age. Furthermore, data quality may be affected by seasonal variability and temporal inconsistencies in satellite imagery. Future research should integrate socio-economic indicators, hydrodynamic variables, and ecological parameters, including vegetation indices combined with mangrove structural characteristics, to develop a more comprehensive assessment of coastal vulnerability and ecosystem-based coastal protection.

A quantitative statistical comparison between the 2015 and 2025 assessments was not performed because the two datasets were derived from different methodological frameworks. The 2015 BNPB assessment represents a government-produced coastal hazard map, whereas the 2025 assessment is based on a field-validated CVI framework integrating remote sensing and GIS. Consequently, the temporal comparison was intended to identify general spatial trends in coastal vulnerability rather than to test statistical differences between datasets. Future studies employing consistent methodologies across multiple observation periods would enable more robust statistical analyses of long-term coastal vulnerability change.

Conclusion

This study demonstrates that integrating the Coastal Vulnerability Index (CVI) with GIS-based spatial analysis provides an effective framework for assessing coastal vulnerability and monitoring its spatial distribution. The results indicate that approximately 70% of the Betahwalang coastal area is currently classified as highly to very highly vulnerable. Comparison with the 2015 BNPB coastal hazard assessment suggests a spatial expansion of vulnerable coastal zones over the past decade, although this comparison should be interpreted qualitatively because the two assessments were developed using different methodologies. Within the adopted CVI framework, geomorphology, coastal slope, and elevation exerted the greatest influence on the final vulnerability classification due to their relatively higher assigned weights. Field observations further suggest that mangrove degradation and extensive aquaculture development may have contributed to greater physical exposure to coastal hazards. The resulting CVI maps provide a scientific basis for vulnerability-based spatial planning, ecosystem-based adaptation, mangrove rehabilitation, and disaster risk reduction. Future research should integrate socio-economic, hydrodynamic, and ecological parameters, together with multi-temporal land-cover analysis, to develop more comprehensive coastal vulnerability assessments.

Acknowledgement

This research was funded by a research grant from Diponegoro University, through the International Publication Research Program under contract number: 222-432/UN7.D2/PP/IV/2025 and also supported by the Regular Fundamental Research Scheme funded by the Ministry of Higher Education, Science, and Technology of the Republic of Indonesia, under research contract No.359-026/UN7.D2.1/PP/V/2025. We would like to express our deep gratitude to the research grant from Diponegoro University, as well as to all the researcher of the Regular Fundamental Research Scheme support to this study. Moreover, we would like to extend our thanks to Integrated Laboratory for Research and Services, Diponegoro University, Semarang, Indonesia for providing research space and their continued institutional support. This study is a testament to the scientific community's collaboration and commitment to advancing our understanding of coastal rehabilitation and disaster mitigation studies. Finally, we would like to thank anonymous reviewers for their revisions and suggestions, which have made this work even more complete.

References

Ariffin, E.H., Mathew, M.J., Roslee, A., Ismailluddin, A., Yun, L.S., Putra, A.B. & Lee, L.H. 2023. A multi-hazards coastal vulnerability index of the East Coast of Peninsular Malaysia. *Int. J. Disaster Risk Reduct.*, 84: 103484. https://doi.org/10.1016/j.ijdrr.2022.10348 4

Arini, D.P., Indarjo, A. & Helmi, M. 2014. Kajian kerentanan pantai di pesisir Kabupaten Rembang Provinsi Jawa Tengah. *J. Mar. Res.*, 3(4): 462–468. https://doi.org/10./jmr.v3 i4.8368

Capobianco, M., de Vriend, H.J., Nicholls, R.J. & Stive, M.J.F. 1999. Coastal area impact and vulnerability assessment: The point of view of a morphodynamic modeller. *J. Coast. Res.*, 15(3): 701–716.

Carvalho, J.L.B., Miranda, I.M., Queiroz, E.V., Guerreiro, J.S., Pereira, H.P. & Vinzon, S.S. 2025. Offshore wave climate of the Pará-Maranhão Basin, Amazonian continental shelf. *Ocean Coast. Res.*, 73: e25007. https://doi.org/10.1590/2675-2824073.2 3129

Darmawan, K., Hani'ah. & Suprayogi, A. 2017. Analisis tingkat kerawanan banjir di Kabupaten Sampang menggunakan metode overlay dengan scoring berbasis Sistem Informasi Geografis. *J. Geod. Undip.*, 6(1): 31–40. https://doi.org/10.14710/jgundip. 2017. 15024

Dewi, R., Zainuri, M., Anggoro, S., Winanto, T. & Endrawati, H. 2017. Characteristic and the distribution of spatio-temporal macronutrient in the lagoon area of Segara Anakan. *Int. J. Mar. Aquat. Resour. Conserv. Coexist.*, 2(1): 51–57.

Ervianto, A. & Hariyanto, B. 2021. Analisis dampak abrasi pantai terhadap lingkungan sosial di Kecamatan Bancar Kabupaten Tuban. *Swara Bhumi*, 1(1): 1–8.

Estradas-Romero, A., Soto, L.A. & Álvarez-Castillo, L. 2025. First determination of photosynthetic pigments in surface sediments from the continental shelf and slope of the northwestern Gulf of Mexico. *Ocean Coast. Res.*, 73: e25008. https://doi.org/10.1590/2675-2824073.2 3175

Fadika, U., Rifai, A. & Rochaddi, B. 2014. Arah dan kecepatan angin musiman serta kaitannya dengan sebaran suhu permukaan laut di Selatan Pangandaran Jawa Barat. *J. Oceanogr.*, 3(3): 429–437.

Fiorucci, M., Martino, S., Della Seta, M., Lenti, L. & Mancini, A. 2022. Seismic response of landslides to natural and man-induced ground vibrations: Evidence from the Petacciato coastal slope (Central Italy). *Eng. Geol.*, 309: 106826. https://doi.org/10.1016/j.enggeo. 2022.106826.

Fithor, A., Prayitno, S.B., Purwanti, F. & Indarjo, A. 2021. Evaluation and application of New-Semarang coastal resources management. *Pertanika J. Sci. Technol.*, 29(3): 1475–1486. https://doi.org/10.47836/pjst.29.3.29

Furlan, E., Pozza, P.D., Michetti, M., Torresan, S., Critto, A. & Marcomini, A. 2021. Development of a multi-dimensional coastal vulnerability index: Assessing vulnerability to inundation scenarios in the Italian coast. *Sci. Total Environ.*, 772: 144650. https://doi.org/10. 1016/j.scitotenv.2020.144650

Gornitz, V. 1991. Global coastal hazards from future sea level rise. *Palaeogeogr.*

Palaeoclimatol. Palaeoecol., 89(4): 379–398. https://doi.org/10.1016/0031-0182(91)90173-O

Hammar, K.E.S., Pendleton, E.A., Thieler, E.R., Williams, S.J. & Norton, G.A. 2003. Coastal vulnerability assessment of Cape Cod National Seashore (CACO) to sea-level rise. *U.S. Geological Survey Open-File Report*, 02-233.

Handayani, E.P., Budihardjo, M.A. & Sugianto, D.N. 2024. Analysis of the application of mangrove rehabilitation structures on mangrove growth and calculation of carbon stocks in the coastal area of Demak, Indonesia. *J. Presipitasi Media Komun. Pengemb. Tek. Lingkung.*, 21(1): 165–173. https://doi.org/10.14710/presipitasi.v21i1.165-173

Hopper, T. & Meixler, M.S. 2016. Modeling coastal vulnerability through space and time. *PLoS One*, 11(10): e0163495. https://doi.org/10.1371/journal.pone.0163495

Irsadi, A., Anggoro, S., Soeprobowati, T.R., Helmi, M. & Khair, A.S.E. 2019. Shoreline and mangrove analysis along Semarang-Demak, Indonesia for sustainable environmental management. *J. Pendidik. IPA Indones.*, 8(1): 1–11. https://doi.org/10.15294/jpii.v8i1.17892

Ledheng, L., Kase, M.S., Hano'e, E.M.Y., Hut, S. & Ling, M. 2024. Isu permasalahan pesisir: Kebencanaan dan kerentanan di wilayah pesisir. Deepublish. ISBN 978-623-02-9698-7.

Macedo, F. & Schettini, C.A. 2025. Observations of the surface current field in morphologically complex environments using drones. *Ocean Coast. Res.*, 73: e25009. https://doi.org/10.1590/2675-2824073.24002

Muliati, Y. 2020. Rekayasa pantai. Bandung: Itenas. ISBN 978-623-7525-29-5.

Ningtias, D.R., Suryono, S. & Susilo, S. 2016. Pengukuran kualitas citra digital computed radiography menggunakan program pengolah citra. *J. Pendidik. Fis. Indones.*, 12(2): 161–168. https://doi.org/10.15294/ jpfi.v12i2.5950

Oktaviani, N. & Kusuma, H.A. 2017. Pengenalan citra satelit Sentinel-2 untuk pemetaan kelautan. *Oseana*, 42(3): 40–55.

Pantusa, D., D'Alessandro, F., Riefolo, L., Principato, F. & Tomasicchio, G.R. 2018. Application of a coastal vulnerability index: A case study along the Apulian coastline, Italy. *Water*, 10(9): 1218. https://doi.org/10.3390/w10091218

Pasomba, T., Jansen, T. & Jasin, M.I. 2019. Analisis karakteristik gelombang daerah Pantai Tobololo Kelurahan Tobololo Kota Ternate Provinsi Maluku Utara. *J. Sipil Statik*, 7(8): 999–1006.

Primasti, T.P.G., Hariyadi, H., Rochaddi, B. & Widada, S. 2021. Pemantauan kerentanan fisik di pesisir Kabupaten Demak (studi kasus perubahan garis pantai). *Indones. J. Oceanogr.*, 3(1): 44–54. https://doi.org/10.14710/ijoce.v3i1.9997

Ramadhany, A.D., Wiranegara, H.W. & Luru, M.N. 2021. Zonasi tingkat kerentanan fisik atas banjir rob Kecamatan Tugu di Kota Semarang. *J. Bhuwana*, 1(2): 137–146. https://doi.org/10.25105/bhuwana.v1i2.12532

Rudiarto, I., Pamungkas, D., Annisa, H. & Adam, K. 2016. Kerentanan sosio-ekonomi terhadap paparan bencana banjir dan rob di pedesaan pesisir Kabupaten Demak. *J. Wil. Lingkung.*, 4(3): 153–170. https://doi.org/10.14710/jwl.4.3.153-170

Sagala, P.M., Bhomia, R.K. & Murdiyarso, D. 2024. Assessment of coastal vulnerability to support mangrove restoration in the northern coast of Java, Indonesia. *Reg. Stud. Mar. Sci.*, 70: 103383. https://doi.org/10.1016/j.rs ma.2024.103383

Sousa, M.B.P.D., Baía, L.B., Martinelli Filho, J.E., Cooper, A. & Ranieri, L.A. 2025. Erosion vulnerability and risk on Amazon estuarine beaches (Marajó Island, Brazil). *Ocean Coast. Res.*, 73: e25005. https://doi.org/10.1590/2675-2824073.24020

Sugianto, D.N. & Muhammad, F. 2019. Mangrove conservation strategy in Bedono Village, Sayung District, Demak Regency based on remote sensing satellite data. *E3S Web Conf.*, 125: 02010. https://doi.org/10.1051/e3sconf/201912502010

Sugianto, D.N., Widiaratih, R., Widada, S., Suripin, Handayani, E.P. & Cahyaningtyas, P. 2022.

Analysis of structural and non-structural disaster mitigation due to erosion in the Timbulsloko Village, Demak–Central Java. *J. Ecol. Eng.*, 23(2): 246–254. https://doi.org/10.12911/22998993/144559

Sugianto, D.N., Purwanto, Handoyo, G., Oktaviani, A., Kunarso, Zainuri, M. & Indarjo, A. 2019. Determination of submerged breakwater location for coastal protection in Panjang Island waters Jepara. *Adv. Sci. Technol. Eng. Syst. J.*, 4(5): 346–351. https://doi.org/10.25046/aj040545.

Sunaryo, S., Ambariyanto, A., Sugianto, D.N., Helmi, M., Kaimuddin, A.H. & Indarjo, A. 2017. Risk analysis of coastal disaster of Semarang City, Indonesia. *E3S Web Conf.*, 31(1): 12009. https://doi.org/10.1051/ e3sconf/20183112009

Suryono, N., Soenardjo, N., Wibowo, E., Ario, R. & Rozy, E.F. 2018. Estimasi kandungan biomassa dan karbon di hutan mangrove Perancak Kabupaten Jembrana, Provinsi Bali. *Bul. Oseanogr. Mar.*, 7(1): 1–8.

Tomasi, M.F. & Klein, A.H.D.F. 2025. Shoreline behavior of beaches adjacent to bay inlet based on satellite imagery analysis. *Ocean Coast. Res.*, 73: e25004. https://doi.org/10.1590/2675-2824073.24073